



ABCG36/PEN3/PDR8 Is an Exporter of the Auxin Precursor, Indole-3-Butyric Acid, and Involved in Auxin-Controlled Development

Bibek Aryal¹, John Huynh¹, Jérôme Schneuwly¹, Alexandra Siffert¹, Jie Liu¹, Santiago Alejandro², Jutta Ludwig-Müller², Enrico Martinoia³ and Markus Geisler^{1*}

¹ Department of Biology, University of Fribourg, Fribourg, Switzerland, ² Institut für Botanik, Technische Universität Dresden, Dresden, Germany, ³ Institute for Plant and Microbial Biology, Zurich, Switzerland

OPEN ACCESS

Edited by:

Joshua Blakeslee,
The Ohio State University,
United States

Reviewed by:

Andrzej Bajguz,
University of Białystok, Poland
Anthony Bishopp,
University of Nottingham,
United Kingdom
Gloria Muday,
Wake Forest University, United States

*Correspondence:

Markus Geisler
markus.geisler@unifr.ch

Specialty section:

This article was submitted to
Plant Traffic and Transport,
a section of the journal
Frontiers in Plant Science

Received: 12 March 2019

Accepted: 25 June 2019

Published: 09 July 2019

Citation:

Aryal B, Huynh J, Schneuwly J,
Siffert A, Liu J, Alejandro S,
Ludwig-Müller J, Martinoia E and
Geisler M (2019)
ABCG36/PEN3/PDR8 Is an Exporter
of the Auxin Precursor,
Indole-3-Butyric Acid, and Involved
in Auxin-Controlled Development.
Front. Plant Sci. 10:899.
doi: 10.3389/fpls.2019.00899

The PDR-type ABCG transporter, ABCG36/PDR8/PEN3, is thought to be implicated in the export of a few structurally unrelated substrates, including the auxin precursor, indole-3-butyric acid (IBA), although a clear-cut proof of transport is lacking. An outward facing, lateral root (LR) location for ABCG36 fuelled speculations that it might secrete IBA into the rhizosphere. Here, we provide strong evidence that ABCG36 catalyzes the export of IBA – but not of indole-3-acetic acid – through the plasma membrane. ABCG36 seems to function redundantly with the closely related isoform ABCG37/PDR9/PIS1 in a negative control of rootward IBA transport in roots, which might be dampened by concerted, lateral IBA export. Analyses of single and double mutant phenotypes suggest that both ABCG36 and ABCG37 function cooperatively in auxin-controlled plant development. Both seem to possess a dual function in the control of auxin homeostasis in the root tip and long-range transport in the mature root correlating with non-polar and polar expression profiles in the LR cap and epidermis, respectively.

Keywords: IBA, IAA, ABCG, ABC transporter, PDR, PEN3, auxin, plant development

INTRODUCTION

Initially, IBA was described as a synthetic auxin that elicited auxin-like effects such as root initiation and was thus used for plant propagation in a process called rooting (reviewed in Frick and Strader, 2018). It has now been established that IBA is an endogenous compound in a variety of plant species examined (Frick and Strader, 2018). Its existence, however, in the model plant *Arabidopsis thaliana* has been questioned (Novak et al., 2012). Currently, it appears that this might simply be a question of extraction and detection methods (Frick and Strader, 2018; Matern et al., 2019). However, until now, it is unclear if IBA acts as an auxin by itself or if it acts strictly via IAA, the major auxin, for which it functions as a precursor (Ludwig-Müller, 2007; Strader and Bartel, 2008; Schlicht et al., 2013). Conversion of IBA to IAA is a peroxisome-dependent

Abbreviations: ABCB, ATP-binding cassette protein subfamily B; ABCG, ATP-binding cassette protein subfamily G; dag, day(s) after germination; dai, day(s) after infection; IAA, indole-3-acetic acid; IBA, indole-3-butyric acid; NPA, 1-N-naphthylphthalamic acid; PAT, polar auxin transport; PDR, pleiotropic drug resistance; PIN, pin-formed; WT, wild-type.

reaction (Zolman et al., 2008) and peroxisomal import is thought to occur by PEROXISOMAL TRANSPORTER1/COMATOSE/ABCD1 (PXA1/CTS/ABCD1) belonging to the ABCD family of ABC transporters (Zolman et al., 2001; Footitt et al., 2002; Hooks et al., 2007).

Indole-3-butyric acid uptake is a saturable process (Rashotte et al., 2003), suggesting that IBA uptake into plant cells is mediated by unidentified IBA uptake carriers (Frick and Strader, 2018; Matern et al., 2019). IBA export is thought to be catalyzed by members of the PDR transporters belonging to the ABCG family of ABC transporters that is limited to plants and fungi (Strader and Bartel, 2009; Kang et al., 2010; Kretzschmar et al., 2012). Interestingly, members of the PIN and ABCB families of IAA transporters do not appear to transport IBA (Ruzicka et al., 2010; Matern et al., 2019) indicating an independent evolution of auxin substrate specificities for distinct transporter classes. Plant PDRs have been assigned to the transport of substrates that are involved in several biotic and abiotic responses: for example, tobacco PDR1 was identified as an exporter of the antifungal terpenoid, sclareol (Jasinski et al., 2001), while PDR5 is induced by the defense hormone, jasmonic acid, and wounding and plays a role in herbicide resistance (Bienert et al., 2012). The PDR, Leaf Rust Resistance34 (Lr34), confers durable, race-specific resistance to multiple fungal pathogens in wheat (Krattinger et al., 2009), while *Petunia* PDR1 has been shown to export the hormone strigolactone in the context of arbuscular mycorrhizal establishment (Kretzschmar et al., 2012).

Mutant alleles of *PDR8/PEN3/ABCG36* (hereafter referred to as ABCG36) were first shown to display altered responses to diverse pathogens (Kobae et al., 2006; Stein et al., 2006), decreased extracellular accumulation of flagellin22-induced callose (Clay et al., 2009) and hyper-accumulation of flagellin22- or pathogen-elicited indole glucosinolate derivatives of the PEN2 pathway (Bednarek et al., 2009; Clay et al., 2009). A striking feature of ABCG36 is its focal accumulation at the site of leaf pathogen entry, where it is thought to export as yet unidentified defense compounds through the plasma membrane (PM) (Stein et al., 2006; Xin et al., 2013). Recently, the indole, 4-methoxyindol-3-yl methanol, was identified as a substrate for ABCG36 functioning in the induced deposition of callose by flagellin22 (Matern et al., 2019).

On the other hand, *abcg36* alleles were found to independently hyper-accumulate and to be hypersensitive to IBA (Strader and Bartel, 2009; Lu et al., 2015). In the root, ABCG36 is predominantly laterally localized at the outermost root PM domains (Langowski et al., 2010; Ruzicka et al., 2010). In these lateral domains, which were defined as the root-soil interface (Langowski et al., 2010; Ruzicka et al., 2010), ABCG36 was shown to co-localize widely with ABCG37 and was thus suggested to act redundantly in mediating root auxin homeostasis (Ruzicka et al., 2010). In agreement, both ABCG36 and ABCG37 were identified in chemical genetic screens for hypersensitivity toward auxinic compounds and auxin transport inhibitors, including IBA (Strader and Bartel, 2009; Ruzicka et al., 2010; Frick and Strader, 2018). Accumulation and reduced efflux from entire root tips were found for different *abcg36* alleles (Strader and Bartel, 2009). Finally, by heterologous expression, ABCG37/PDR9/PIS1 was

shown to function as a transporter of IBA and 2,4-D but not of IAA (Ruzicka et al., 2010). In summary, genetic and biochemical approaches in Arabidopsis support the idea that IBA efflux from root cells is catalyzed by at least two PDRs of the ABCG family of ABC transporters, ABCG36/PDR8/PEN3 (Strader and Bartel, 2009; Lu et al., 2015) and ABCG37/PDR9/PIS1 (Strader et al., 2008; Ruzicka et al., 2010). IBA hypersensitivity phenotypes of mutants defective in these transporters suggest that IBA is a common substrate exported by both ABCG36 and ABCG37 (Strader and Bartel, 2009) but clear IBA transport data have so far only been provided for ABCG37 (Ruzicka et al., 2010).

Here we provide strong evidence that ABCG36 functions as a PM exporter of IBA that dampens polar (rootward) IBA transport in the root. Further, our data support a functional interplay with ABCG37 in auxin-controlled plant physiology.

MATERIALS AND METHODS

Plant Material and Phenotypic Analyses

The following *Arabidopsis thaliana* lines in ecotype Columbia (Col Wt) were used: *abcg36-4 (pen3-4)* (Stein et al., 2006), *abcg37-2 (pdr9-2)* (Ito and Gray, 2006), *abcg36-4 abcg37-2 (pen3-4 pdr9-2)* (Ruzicka et al., 2010), *35S:ABCG37-GFP (35S:PIS1-GFP)* (Ruzicka et al., 2010), *ABCG36:ABCG36-GFP (PEN3:PEN3-GFP)* (Stein et al., 2006). *DR5:GFP* (Ottenschlager et al., 2003), was crossed into *abcg36-4* and *abcg37-2* and isogenic, homozygous lines for the transgene in the F3 generations were used for further analyses. *35S:ABCG36* Arabidopsis lines were constructed by transforming *35S:PDR8* (Kim et al., 2007) into the *abcg36-4/pen3-4* mutant.

Seedlings were generally grown on vertical plates containing 0.5 Murashige and Skoog media, 1% sucrose, and 0.75% phytoagar in the dark or at 16 h (long day) light per day. Developmental parameters, such as primary root lengths, lateral root (LR) number and root gravitropism, primary root and hypocotyl elongation were quantified from scanned plates using the Fiji plugin¹ for ImageJ². All experiments were performed at least in triplicate with 30 to 40 seedlings per experiment.

Yeast Work

cDNA of ABCG36 was PCR-amplified and inserted into BamHI/XhoI sites of pYES2NT/C-ABCG36. ABCG36 and ABCG37 were expressed from shuttle vectors pYES2NT/C-ABCG36, pNEV-ABCG37-HA (Ruzicka et al., 2010) in Wt strain JK93da (Hemenway and Heitman, 1996). Yeast IBA/2,4-D transport was performed as described (Kim et al., 2010).

Confocal Laser Scanning Imaging

For confocal laser scanning microscopy work, a SP5 confocal laser microscope was used. Confocal settings were set to record the emission of GFP (excitation 488 nm, emission 500–550 nm) and FM4-64 (excitation 561 nm, emission 600–680 nm).

¹<https://imagej.net/Fiji>

²<https://imagej.net>

Plant Auxin Transport

Simultaneous export of [ring-³H]-IBA (specific activity 25 Ci mmol⁻¹; American Radiolabeled Chemicals, ART1112) with either [carboxyl-¹⁴C]-2,4-D (specific activity 50 mCi mmol⁻¹; American Radiolabeled Chemicals, ARC0722) or [1-¹⁴C]-IAA (specific activity 55 mCi mmol⁻¹; American Radiolabeled Chemicals, ARC1060) from *Arabidopsis* and *Nicotiana benthamiana* mesophyll protoplasts was analyzed as described (Henrichs et al., 2012). *N. benthamiana* mesophyll protoplasts were measured 4 days after *Agrobacterium*-mediated transfection of 35S:ABCG36/35S:PDR8 (Kim et al., 2007) or 35S:ABCG37-GFP (Ruzicka et al., 2010). In short, after loading, external radioactivity was removed by separating protoplasts in a 50-30-5% Percoll gradient. Transport was initiated by incubation at 25°C and halted by silicon oil centrifugation. Exported radioactivity was determined by scintillation counting of aqueous phases and is presented as the relative efflux of the initial efflux (efflux prior to temperature incubation), which was set to zero. Relative export from protoplasts was calculated from exported radioactivity into the supernatant as follows: (radioactivity in the supernatant at time t = x min) – (radioactivity in the supernatant at time t = 0) * (100%)/(radioactivity in the supernatant at t = 0 min); mean values are presented from four independent experiments. Rootward (acropetal) and shootward (basipetal) PAT in roots was measured as described in Lewis and Muday (2009).

In planta Analysis of Auxin Contents and Responses

Endogenous free IBA and IAA were quantified from shoot and root segments of 9-days-after-germination (dag) light-grown (16 h) *Arabidopsis* seedlings by using gas chromatography-mass spectrometry (GC-MS) as described in Leljak-Levanic et al. (2010). Methylation was performed by adding equal sample amounts of a 1:10 diluted solution (in diethylether) of trimethylsilyldiazomethane solution (Sigma-Aldrich) for 30 min at room temperature. The mixture was then evaporated and resuspended in 50 µl of ethyl acetate for GC-MS analysis. Data are means of four independent lots of 30–50 seedlings each, and equivalent to ca. 100 mg root shoot material, respectively.

Homozygous generations of *Arabidopsis abcg36-4* and *abcg36-4 abcg37-2* expressing DR5:GFP were obtained by crossing with DR5:GFP lines (Ottenschlager et al., 2003). Seedlings were grown vertically for 5 (dag) and then for 4 h on 5 (M IBA plates and analyzed by confocal laser-scanning microscopy. DR5:GFP signals in the very root tip were analyzed using the Fiji software³.

Data Analysis

Data were statistically analyzed using Prism 7.0a (GraphPad Software, San Diego, CA, United States) and the R software package of the Comprehensive R Archive Network (CRAN)⁴.

³<https://imagej.net/Fiji>

⁴<http://cran.r-project.org>

RESULTS

ABCG36 Functions as an Exporter of IBA

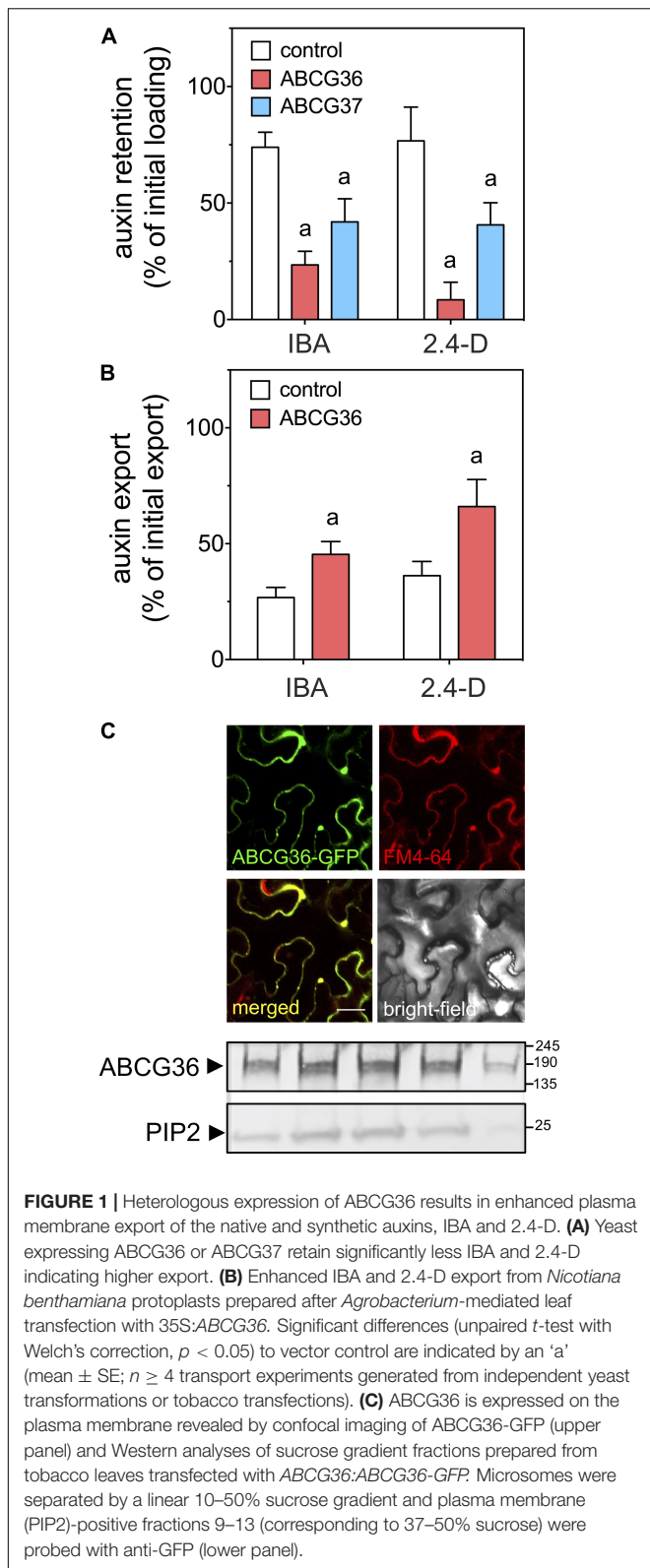
Recently, by heterologous expression in yeast and HeLa cells, ABCG37/PDR9/PIS1 was shown to function as a transporter of IBA, 2,4-D and NPA but not of IAA (Ruzicka et al., 2010). For different *abcg36* alleles, increased accumulation and reduced efflux from entire root tips were measured (Strader and Bartel, 2009) but no direct transport data, especially in the absence of plant-specific factors, was provided.

In order to demonstrate such a transport activity, we functionally expressed ABCG36 in the heterologous, non-plant and plant systems, baker's yeast and tobacco (*N. benthamiana*), respectively. ABCG36- and ABCG37-expressing yeast (the latter was used here as a positive control) revealed significantly reduced retention of IBA and 2,4-D, assayed in parallel by double isotope labeling (Figure 1A). Reduced retention argues for an export activity. *N. benthamiana* transfection resulted in expression of ABCG36 at the PM of epidermal cells as was shown by co-localization with FM-4-64 after short-term incubation of transfected leaves (Figure 1C). Confocal imaging was verified biochemically by demonstrating co-sedimentation of ABCG36-positive microsomal fractions with the PM marker, PIP2;1, using Western blotting after fractionation on a linear sucrose gradient. ABCG36 expression on the PM greatly enhanced IBA and 2,4-D export from prepared tobacco protoplasts (Figure 1B) as was shown before for ABCG37 (Ruzicka et al., 2010).

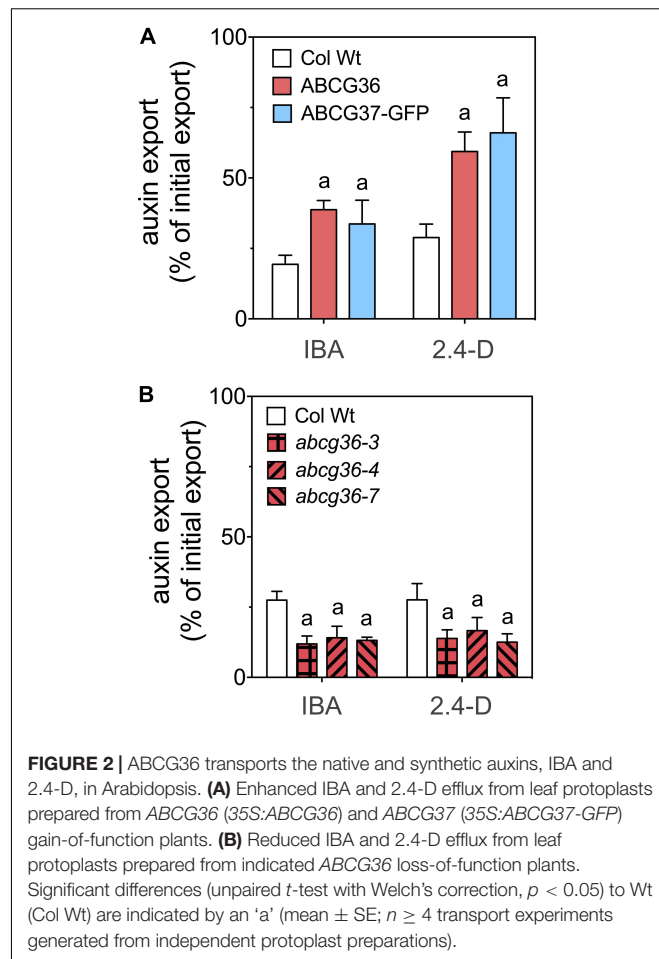
Next, we quantified IBA/2,4-D export from stable *Arabidopsis* lines over-expressing ABCG36 (Kim et al., 2007) and ABCG37-GFP (Ruzicka et al., 2010). Both lines exported significantly more IBA and 2,4-D (Figure 2A) but not IAA (Supplementary Figure 1) compared to the corresponding Wt. In agreement, T-DNA insertion, null alleles of ABCG36, *abcg36-3*, *abcg36-4*, *abcg36-7*, previously shown to express no ABCG36 protein (Lu et al., 2015), revealed significantly reduced IBA and 2,4-D export (Figure 2B). In summary, these data verify a PM export activity of ABCG36 for IBA but additionally indicate a high degree of substrate specificity as was already found for ABCG37 (Ruzicka et al., 2010).

ABCG36 Functions in the Polar Distribution of IBA

Previous work has established that in roots both IBA and IAA both move with distinct polarities at similar transport rates (Rashotte et al., 2003). Inspired by the striking polar expression of ABCG36 and ABCG37 in the root epidermis (Ruzicka et al., 2010; Mao et al., 2016; see Figure 3C) and in order to demonstrate an involvement of ABCG36 in this process, we quantified polar IBA and IAA transport in 5 mm segments from the source. Both radiotracers were applied to root-shoot junctions and root tips by diffusion into plant tissues from agar beads functioning as source (Lewis and Muday, 2009). Results revealed to our surprise that rootward (acropetal) transport is enhanced in *abcg36*, *abcg37* and *abcg36 abcg37* mutant roots, although significant differences were only found

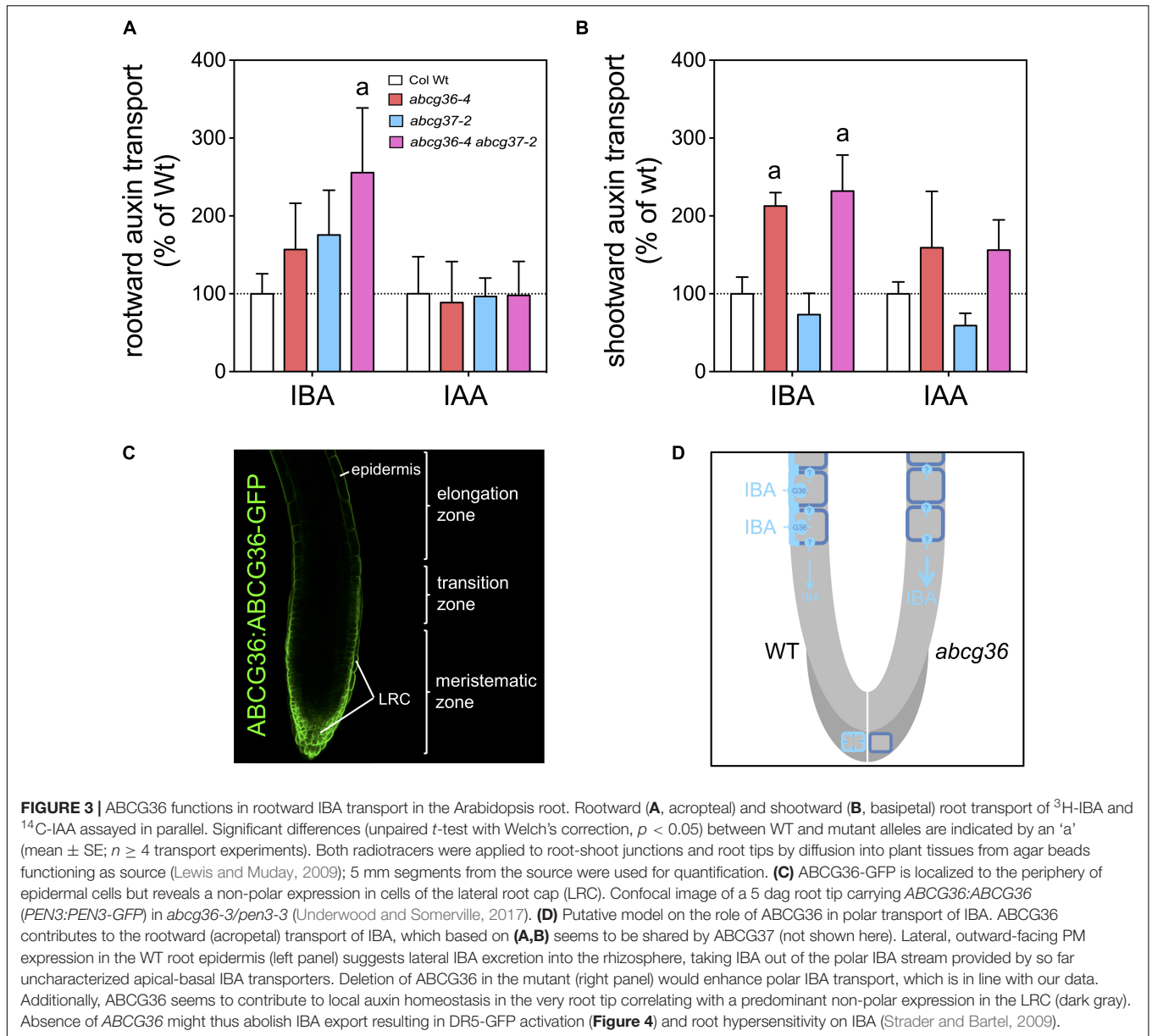


with the double mutant (**Figure 3A**). This effect is specific for IBA as it was not found with IAA assayed simultaneously. Shootward (basipetal) transport rates were likewise significantly



enhanced in *abcg36* and *abcbg36 abcbg37* but not in *abcg37* roots, which might indicate a selective contribution of ABCG37 in this transport stream. Slightly reduced, although not significant, shootward transport in *abcg37* roots is in agreement with a recent report (Ruzicka et al., 2010), however, it is important to mention that application methods employed differ. While we here applied radiolabeled IAA by placing agar beads containing low amount of radiotracers next to the plant tissue (Lewis and Muday, 2009), Ruzicka et al. (2010) used direct nano-droplet application to the plant tissues, which might result in external passage of auxin-containing microfluids by capillary forces.

Enhanced rootward and shootward transport rates for ABCG36/37 transporter loss-of-function mutants might seem counter-intuitive at first sight. In light of the strict lateral, outward-facing distribution for ABCG36 (Strader and Bartel, 2009, see **Figure 3C**) and ABCG37 (Ruzicka et al., 2010) in the region that is relevant for this transport measurement, a plausible explanation is that both transporters might function in lateral exclusion of IBA from the apical-basal transport stream. Loss-of-function would thus result in enhanced polar IBA transport (see **Figure 3D**). Altogether, this dataset further substantiates that ABCG36 like ABCG37 acts as an IBA exporter and is involved in the regulation of its polar



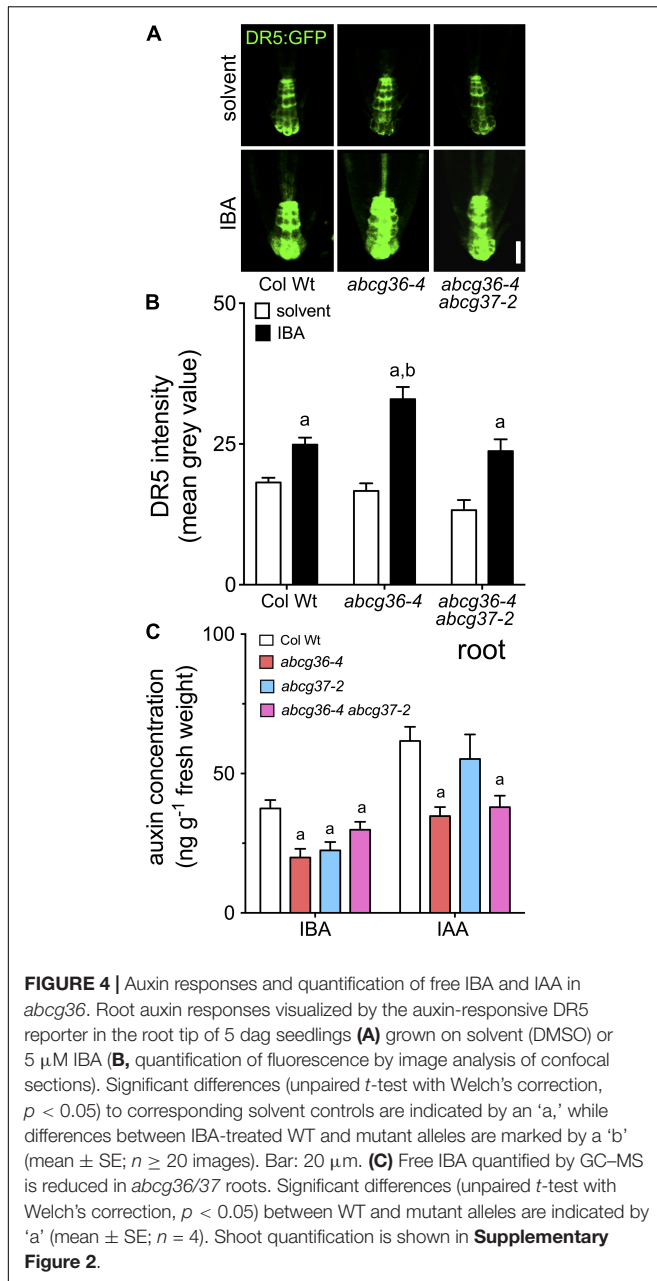
distribution by a yet unidentified apical-basal transport machinery (Figure 3D).

ABCG36 and ABCG37 Have an Impact on Auxin Signaling and Accumulation

Recently, hyper-sensitivity of *abcb37-1/pis1-1* roots to IBA was correlated with increased induction of the auxin (IAA) signaling reporter, DR5:GFP, known to be not activated by IBA itself (Ruzicka et al., 2010). Based on quantification of DR5:GFP expression in the root tip, auxin signaling was not found to be different in *abcb36-4* and *abcb36-4 abcb37-2* compared to WT on control media (Figures 4A,B), as shown for *abcb37-1/pis1-1* (Ruzicka et al., 2010). However, like *abcb37-1* (Ruzicka et al., 2010), application of IBA led to significantly higher reporter

activation in the *abcb36-4* columella cells compared to the WT, and results in additional signals in the stele (Figures 4A,B). Interestingly, this effect was reverted in the *abcb36-4 abcb37-2* double mutant to Wt level arguing for compensating roles of both transporters in the columella cells (see section "Discussion").

In order to provide more direct evidence for an involvement of ABCG36 (and ABCG37) in IBA/IAA homeostasis and to dissect IBA and IAA – but also ABCG36,37 – functionalities, we analyzed free IBA and IAA levels from entire root and shoot segments of Arabidopsis seedlings by GC-MS. Both roots and shoots of *abcb36* and *abcb37* single and double mutants contained significantly less IBA than the WT most likely caused by defects in apical-basal IBA distribution (Figure 4C and Supplementary Figure 2). Interestingly, IAA levels in *abcb36-4* and *abcb36-4 abcb37-2* roots – but not in those of *abcb37-2* – were also reduced,



which is in line with enhanced polar transport rates for IBA (Figure 3). In summary, this data set uncovers that ABCG36 and ABCG37 have both an impact on root and shoot IBA and IAA homeostasis but that their individual impact is tissue-specific.

ABCG36 Is Involved in Some – But Not All – Auxin-Controlled Developmental Programs in an Action That Is Partly Shared With ABCG37

Originally, the ABCG36 allele, *abcg36-6/pdr8-115*, was isolated in a screen for mutants that were able to restore IBA but not IAA responsiveness to auxin signaling mutants (Strader and

Bartel, 2009). In the following, individual mutant alleles of ABCG36 were tested for their sensitivity toward IBA using root growth as read-out but different technical setups revealed mixed reports: while *abcg36-1/pen3-1*, *abcg36-2/pen3-2*, *abcg36-3-pen3-3*, *abcg36-4/pen3-4*, and *abcg36-6* were found to be hypersensitive (Ruzicka et al., 2010; Strader and Bartel, 2011; Lu et al., 2015), the point mutation allele, *abcg36-5*, was not (Lu et al., 2015). For the *abcg37-2/pdr9-2* allele, hypersensitivity toward IBA as well as a redundant function with ABCG36 were reported (Ruzicka et al., 2010).

We therefore re-analyzed the performance of an established set of ABCG36 and ABCG37 single and double loss-of-function lines (Ruzicka et al., 2010) in respect to well-characterized, auxin-controlled growth programs. In order to be able to potentially dissect the role of individual ABCG-type transporters in IBA homeostasis, we also quantified seedling phenotypes after transfer to IBA plates. While hypocotyls at standard conditions (22°C) had no obvious phenotypes, growth at 28°C – known to cause a shift to thermomorphogenesis characterized by elongated hypocotyls most likely triggered by enhanced IAA (Gray et al., 1998; Gil and Park, 2019) – greatly reduced hypocotyl elongation in the order *abcg36 < abcg37 < abcg36 abcg37* in comparison to WT (Figure 5A). IBA enhanced this phenotype at 28°C but not at 22°C suggesting that increased conversion of IBA to IAA might be responsible for this effect. Analysis of hook opening in etiolated seedlings, another hallmark of auxin-regulated shoot development (Abbas et al., 2013), revealed that single ABCG36 or ABCG37 mutation did not significantly affect hook opening angles, while the *abcg36-4 abcg37-2* double mutant revealed an impaired hook opening angle (Figure 5B). IBA treatment generally inhibited hook opening compared to the solvent control but also ameliorated the differences between the mutant alleles.

Results for root elongation indicated that *abcg36-4* and *abcg37-2* roots elongate faster on solvent plates as was previously found (Strader and Bartel, 2009; Ruzicka et al., 2010), while this phenotype is lost in *abcg36-4 abcg37-2* (Figure 5C). As found for hook opening, IBA inhibited root elongation overall. As shown before *abcg36-4 abcg37-2* was hypersensitive in comparison to Wt (Ruzicka et al., 2010), while *abcg36-4* and *abcg37-2/pdr9-2* was not. The latter is in agreement with a former report (Ito and Gray, 2006) who likewise employed a transfer of seedlings onto IBA medium, while apparently, growth on IBA produces different results (Ruzicka et al., 2010). As a second developmental root parameter, we measured the number of emerged LR. Again, it was found that *abcg36-4* roots produce slightly more LR (cf Strader and Bartel, 2009). According to its known rooting potential, IBA increased LR numbers for all accessions tested, and the *abcg36-4* allele was clearly hyper-responsive toward IBA (Strader and Bartel, 2009), while ABCG37 mutant combinations were not (Figure 5D). As a last physiological constraint, we measured root gravitropism for the same mutant set, which to our knowledge has not been analyzed in this respect. In contrast to most measured read-outs, all ABCG36 and ABCG37 loss-of-function alleles revealed Wt-like root bending (Figure 5E). Also, all mutant lines showed similar sensitivities toward the non-competitive auxin transport inhibitor, *N*-1-naphthylphthalamic acid (NPA; see Figure 5F), that efficiently blocks IAA-controlled

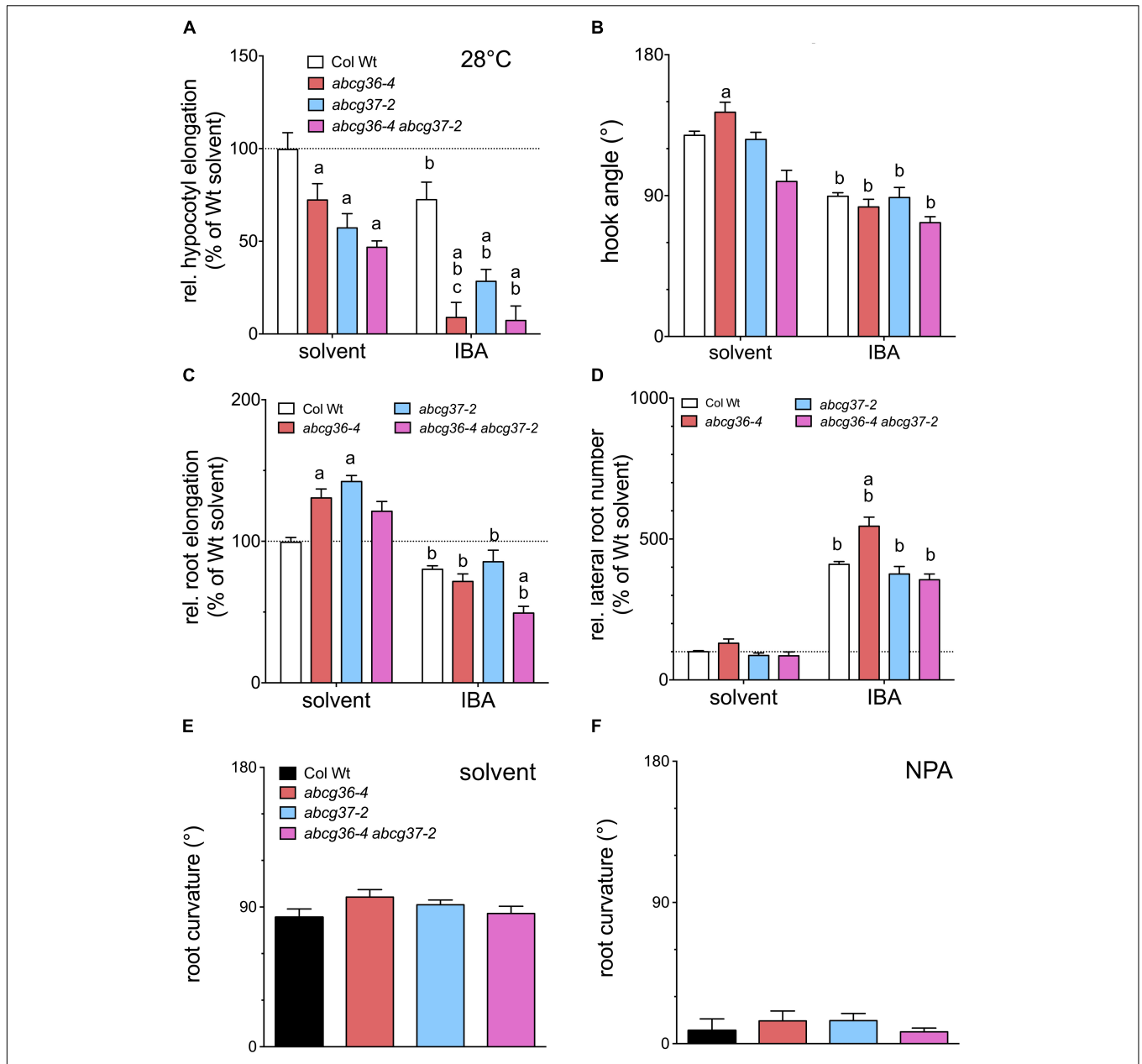


FIGURE 5 | ABCG36 contributes to auxin-controlled plant development. **(A)** Hypocotyl elongation of 5 dag seedlings after transfer onto solvent control or IBA (5 μ M) plates after 3 days at 28°C. 22°C control is shown in **Supplementary Figure 3**. **(B)** Hook opening angle of etiolated seedlings grown for 3 days in the dark and transferred onto solvent control or IBA (5 μ M) plates in the dark after 4 days. **(C)** Root elongation of 5 dag seedlings after transfer onto solvent control or IBA (5 μ M) plates after 24 h. **(D)** Quantification of emerged lateral roots of 5 dag seedlings after transfer onto solvent control or IBA (5 μ M) plates after 7 days. Significant differences (unpaired *t*-test with Welch's correction, $p < 0.05$) between corresponding WT and mutant alleles are marked with an 'a,' differences to corresponding WT solvent control with a 'b' (means \pm SE; $n = 4$ sets of > 20 seedlings each). For root bending assays, 5 dag seedlings were transferred to solvent control **(E)** or NPA (10 μ M) plates **(F)**, and root bending angles were judged after 12 h in the dark.

root gravitropism (Bailey et al., 2008). The finding that *abcg* mutant roots bend like Wt on NPA might indicate that both transporters are not sensitive to NPA as was suggested before for IBA transport in general (Liu et al., 2012).

In summary, these data support an involvement of ABCG36 in most of the auxin-controlled developmental programs tested, such as hypocotyl and root elongation and hook opening. This

action of ABCG36 is partly shared with ABCG37, as illustrated by hypocotyl elongation and hook opening. However, root gravitropism data suggest that ABCG36 (and ABCG37) is not involved in all auxin-controlled processes. Our analyses also revealed that IBA altered all four of the developmental read-outs tested. Amongst those, hypersensitivity of ABCG36/37 mutant alleles to IBA (as for hypocotyl elongation, root elongation and

LR development; **Figure 5**) further supports the involvement of ABCG36/37 in auxin-controlled development.

DISCUSSION

ABCG36 Is an IBA Exporter Negatively Regulating Rootward IBA Transport

The current work enhances the portfolio of ABCG36 substrates by the auxin precursor, IBA. This has been established by heterologous expression in non-plant (yeast) and plant systems (tobacco; **Figure 1**). Recently, expression of ABCG37 in yeast resulted in mislocation to the ER leading to enhanced yeast loading (Ruzicka et al., 2010). Using an identical approach and even the same construct for ABCG37, we here report PM export for ABCG36 and ABCG37; discrepancies in localizations for ABCG37 in yeast between Ruzicka et al. (2010) and this study are currently not known. However, PM exports of IBA (and 2,4-D) were verified in tobacco and *in vivo* by analyses of Arabidopsis ABCG36 gain- and loss-of-function mutant lines (**Figures 1, 2**).

It appears that ABCG36 and ABCG37 apparently possess a wider, but clearly delimited, specificity for a few overlapping but structurally unrelated substrates found to be typical for PDR-type ABC transporters (Kang et al., 2010; Borghi et al., 2015). However, it should be mentioned that the substrate sets described are not identical: ABCG37 but not ABCG36 was found to transport phenolic compounds, including coumarin (Fourcroy et al., 2014, 2016; Ziegler et al., 2017). Interestingly, in this substrate category, ABCG36 (like ABCG37) seems to be specific for a few auxinic compounds, such as IBA and 2,4-D, but both do not, for example, transport the major native auxin, IAA (**Supplementary Figure 1**), which only differs from IBA by a two-carbon chain. A future venue for this interesting finding might be offered by the *abcg36-5/pen3-5* allele that was reported to uncouple ABCG36 function in IBA-stimulated root growth, callose and a pathogen-inducible accumulation of salicylic acid from ABCG36 activity in extracellular defense (Lu et al., 2015).

Previous reports left us with a certain degree of uncertainty if IBA is indeed transported in a polar fashion (Rashotte et al., 2003; Ruzicka et al., 2010; Liu et al., 2012). While Rashotte et al. (2003) provided evidence for polar IBA transport in the shoot and roots without analyzing the radiotracer, Liu et al. (2012) clearly demonstrated polar IBA movement, distinct from that of IAA in the hypocotyl. In contrast, Ruzicka et al. (2010) demonstrated that already after 2 h most of the IBA applied to roots is metabolized into IAA. Our careful analysis of PAT in Arabidopsis roots revealed that ABCG36 functions redundantly with ABCG37 in rootward IBA (but not IAA) transport (**Figure 3A**). As discussed above, their role seems to lie in diminishing rootward IAA streams provided by so far unknown IBA transporters, by concerted, lateral IBA export out of the root (**Figure 3D**). Enhanced rootward, long-range IBA transport leads apparently to reduced concentrations of free IBA in *abcg36-4* and *abcg37-2*, measured here over entire roots. Although a final proof of lateral, epidermal ABCG36/37-mediated IBA export is lacking due to technical limitations, the

overall concept is in agreement with increased accumulation and reduced efflux from *abcg36* root tips (Strader and Bartel, 2009).

At first view, ABCG36 (but not ABCG37) also seems to have a negative impact on shootward transport of IBA in the root (**Figure 3B**). However, shootward IAA transport profiles remarkably resemble those of IBA, although both ABCG transporters were shown not to transport IAA (**Figure 3B**; Ruzicka et al., 2010). Therefore, we cannot exclude that differences in shootward IAA transport might be caused by peroxisomal conversion of ring-labeled IBA to IAA during the elevated time-frame that is technically necessary for measuring this slow directionality (18 h for shootward vs. 3 h for rootward transport). Although the impact of IBA-to-IAA conversion in Arabidopsis roots has been discussed controversially (Ruzicka et al., 2010; Liu et al., 2012), we believe that polar root transport of IBA using radiotracers can only be safely quantified in a rootward direction.

In contrast to direct IBA/IAA quantifications of entire roots, signals of the columella, maximum IAA reporter, DR5:GFP, were unchanged in *abcg36-4* and *abcg36-4 abcg37-2* on solvent control, as found for *abcg37-2* (Ruzicka et al., 2010). In analogy, IBA significantly enhanced reporter expression compared to Wt in *abcg36-4* (**Figures 4A,B**), most likely by IBA to IAA conversion caused by lack of LRC export. In summary, these data support a dual function of ABCG36 in the polar (rootward) distribution of IBA in the root and local IBA/IAA homeostasis in the very root tip. These features correlate with the mainly polar (lateral) expression pattern in the mature root and a widely non-polar expression in the LR cap cells (see **Figure 3D**; Strader and Bartel, 2009; Ruzicka et al., 2010; Mao et al., 2016, 2017).

ABCG36 and ABCG37 Are Partly Redundant

Widely overlapping substrate profiles and PM localizations between ABCG36 and ABCG37 imply but do not directly prove functional redundancy. A meta-analysis of our data supports the concept that ABCG36 and ABCG37 indeed function at least partly redundantly. This is confirmed by analyses of hook opening, of hypocotyl elongation at 28°C and of root elongation in the presence of exogenous IBA (**Figure 5**). Leaving uncertain or indirect observations, like shootward PAT of IBA or DR5-GFP reporter activation, aside, a few other read-outs do not support a common function in the same pathway. For example, LR development that is enhanced with IBA in *abcb36-4* (**Figure 5D**; Strader and Bartel, 2009) seems to be independent of ABCG37. This is surprising because LRs are thought to be initiated by a shoot-derived auxin maximum (Casimiro et al., 2003; Schlicht et al., 2013), and based on our data, shootward IBA root transport is apparently provided by both ABCG36 and ABCG37 (**Figures 4, 5**).

Interestingly, quantification of auxin responses, free IBA and root elongation in *abcg36 abcg37* roots (**Figure 2**), revealed a certain degree of compensation of individual single-mutant phenotypes. In light of an overall redundant function in IBA transport this is not easy to understand. An important finding in this respect might be that ABCG37 was found to be a frequent

interactor of ABCG36 (Aryal and Geisler, unpublished). An appealing scenario is therefore that ABCG36 and ABCG37 itself functionally interact, which might explain both the discrepancies found during compensatory and redundant function. The impact of full-size ABC-ABC transporter interaction is currently still unclear but has been recently supported by uncovering the ABC transporter interactome in yeast (Snider et al., 2013).

Analyses of *abcg36/37* Mutants Allowed to Partially Dissect the Roles of IBA and IAA Transport Pathways

The analyses presented here for *abcg36/37* mutants in respect to auxin-controlled growth processes allowed us to partially dissect the roles of IBA and IAA transport pathways and their involvement in either IBA or IAA-controlled plant development. As pointed out above, all of the growth parameters investigated were affected by IBA (Figure 5). More interestingly, *abcg36/37* mutants were hypersensitive to IBA in all four of the tested developmental read-outs, although to different degrees (Figure 5): while this effect seems to be specific for ABCG36 during hypocotyl elongation and LR initiation (Figures 5A,D), this functionality seems to be shared with ABCG37 during root elongation. A concerted action of ABCG36 with ABCG37 contributes to the polar (rootward) distribution of IBA in the plant root and is responsible for auxin-controlled development.

DATA AVAILABILITY

All datasets generated for this study are included in the manuscript and/or the **Supplementary Files**.

REFERENCES

- Abbas, M., Alabadi, D., and Blazquez, M. A. (2013). Differential growth at the apical hook: all roads lead to auxin. *Front. Plant Sci.* 4:441. doi: 10.3389/fpls.2013.00441
- Bailly, A., Sovero, V., Vincenzetti, V., Santelia, D., Bartnik, D., Koenig, B. W., et al. (2008). Modulation of P-glycoproteins by auxin transport inhibitors is mediated by interaction with immunophilins. *J. Biol. Chem.* 283, 21817–21826. doi: 10.1074/jbc.M709655200
- Bednarek, P., Pislewska-Bednarek, M., Svatos, A., Schneider, B., Doudsky, J., Mansurova, M., et al. (2009). A glucosinolate metabolism pathway in living plant cells mediates broad-spectrum antifungal defense. *Science* 323, 101–106. doi: 10.1126/science.1163732
- Bienert, M. D., Siegmund, S. E., Drozak, A., Trombik, T., Bultreys, A., Baldwin, I. T., et al. (2012). A pleiotropic drug resistance transporter in *Nicotiana tabacum* is involved in defense against the herbivore *Manduca sexta*. *Plant J.* 72, 745–757. doi: 10.1111/j.1365-313X.2012.05108.x
- Borghii, L., Kang, J., Ko, D., Lee, Y., and Martinoia, E. (2015). The role of ABCG-type ABC transporters in phytohormone transport. *Biochem. Soc. Trans.* 43, 924–930. doi: 10.1042/BST20150106
- Casimiro, I., Beeckman, T., Graham, N., Bhalerao, R., Zhang, H. M., Casero, P., et al. (2003). Dissecting *Arabidopsis* lateral root development. *Trends Plant Sci.* 8, 165–171. doi: 10.1016/s1360-1385(03)00051-7
- Clay, N. K., Adio, A. M., Denoux, C., Jander, G., and Ausubel, F. M. (2009). Glucosinolate metabolites required for an *Arabidopsis* innate immune response. *Science* 323, 95–101. doi: 10.1126/science.1164627
- Footitt, S., Slocombe, S. P., Larner, V., Kurup, S., Wu, Y., Larson, T., et al. (2002). Control of germination and lipid mobilization by COMATOSE, the *Arabidopsis*

AUTHOR CONTRIBUTIONS

MG and BA designed the research. BA, JS, JH, AS, JL-M, and JL performed the research. SA and EM provided unpublished material. BA, JS, JH, JL-M, and MG analyzed the data. MG wrote the manuscript.

FUNDING

This work was supported by grants from the Swiss National Funds (31003A-165877/1), the *Pool de Recherche* of the University of Fribourg and the ESA (CORA grant LIRAT) (all to MG).

ACKNOWLEDGMENTS

We would like thank L. Charrier for excellent technical assistance, J. Friml for *35S:ABCG37-GFP*, *abcg36-2/pdr9-2*, *abcg36-4/pen3-4*, and *abcg37-2/pdr9-2* lines, B. Underwood for the *PEN3:PEN3-GFP* plasmid construct, R. Rohr and L.-F. Bersier for help with statistical analyses and Antony Buchala for discussion and language editing of the manuscript.

SUPPLEMENTARY MATERIAL

The Supplementary Material for this article can be found online at: <https://www.frontiersin.org/articles/10.3389/fpls.2019.00899/full#supplementary-material>

- homologue of human ALDP. *EMBO J.* 21, 2912–2922. doi: 10.1093/emboj/cdf300
- Fourcroy, P., Siso-Terraza, P., Sudre, D., Saviron, M., Reyt, G., Gaymard, F., et al. (2014). Involvement of the ABCG37 transporter in secretion of scopoletin and derivatives by *Arabidopsis* roots in response to iron deficiency. *New Phytol.* 201, 155–167. doi: 10.1111/nph.12471
- Fourcroy, P., Tissot, N., Gaymard, F., Briat, J. F., and Dubos, C. (2016). Facilitated Fe nutrition by phenolic compounds excreted by the *Arabidopsis* ABCG37/PDR9 transporter requires the IRT1/FRO2 high-affinity root Fe(2+) transport system. *Mol. Plant* 9, 485–488. doi: 10.1016/j.molp.2015.09.010
- Frick, E. M., and Strader, L. C. (2018). Roles for IBA-derived auxin in plant development. *J. Exp. Bot.* 69, 169–177. doi: 10.1093/jxb/erx298
- Gil, K. E., and Park, C. M. (2019). Thermal adaptation and plasticity of the plant circadian clock. *New Phytol.* 221, 1215–1229. doi: 10.1111/nph.15518
- Gray, W. M., Ostin, A., Sandberg, G., Romano, C. P., and Estelle, M. (1998). High temperature promotes auxin-mediated hypocotyl elongation in *Arabidopsis*. *Proc. Natl. Acad. Sci. U.S.A.* 95, 7197–7202. doi: 10.1073/pnas.95.12.7197
- Hemenway, C. S., and Heitman, J. (1996). Immunosuppressant target protein FKBP12 is required for P-glycoprotein function in yeast. *J. Biol. Chem.* 271, 18527–18534. doi: 10.1074/jbc.271.31.18527
- Henrichs, S., Wang, B., Fukao, Y., Zhu, J., Charrier, L., Bailly, A., et al. (2012). Regulation of ABCB1/PGP1-catalysed auxin transport by linker phosphorylation. *EMBO J.* 31, 2965–2980. doi: 10.1038/emboj.2012.120
- Hooks, M. A., Turner, J. E., Murphy, E. C., Johnston, K. A., Burr, S., and Jaroslowski, S. (2007). The *Arabidopsis* ALDP protein homologue COMATOSE is instrumental in peroxisomal acetate metabolism. *Biochem. J.* 406, 399–406. doi: 10.1042/BJ20070258

- Ito, H., and Gray, W. M. (2006). A gain-of-function mutation in the *Arabidopsis* pleiotropic drug resistance transporter PDR9 confers resistance to auxinic herbicides. *Plant Physiol.* 142, 63–74. doi: 10.1104/pp.106.084533
- Jasinski, M., Stukkens, Y., Degand, H., Purnelle, B., Marchand-Brynaert, J., and Boutry, M. (2001). A plant plasma membrane ATP binding cassette-type transporter is involved in antifungal terpenoid secretion. *Plant Cell* 13, 1095–1107. doi: 10.1105/tpc.13.5.1095
- Kang, J., Hwang, J. U., Lee, M., Kim, Y. Y., Assmann, S. M., Martinoia, E., et al. (2010). PDR-type ABC transporter mediates cellular uptake of the phytohormone abscisic acid. *Proc. Natl. Acad. Sci. U.S.A.* 107, 2355–2360. doi: 10.1073/pnas.0909222107
- Kim, D. Y., Bovet, L., Maeshima, M., Martinoia, E., and Lee, Y. (2007). The ABC transporter AtPDR8 is a cadmium extrusion pump conferring heavy metal resistance. *Plant J.* 50, 207–218. doi: 10.1111/j.1365-313X.2007.03044.x
- Kim, J. Y., Henrichs, S., Bailly, A., Vincenzetti, V., Sovero, V., Mancuso, S., et al. (2010). Identification of an ABC/P-glycoprotein-specific inhibitor of auxin transport by chemical genomics. *J. Biol. Chem.* 285, 23309–23317. doi: 10.1074/jbc.M110.105981
- Kobae, Y., Sekino, T., Yoshioka, H., Nakagawa, T., Martinoia, E., and Maeshima, M. (2006). Loss of AtPDR8, a plasma membrane ABC transporter of *Arabidopsis thaliana*, causes hypersensitive cell death upon pathogen infection. *Plant Cell Physiol.* 47, 309–318. doi: 10.1093/pcp/pcj001
- Krattinger, S. G., Lagudah, E. S., Spielmeier, W., Singh, R. P., Huerta-Espino, J., McFadden, H., et al. (2009). A putative ABC transporter confers durable resistance to multiple fungal pathogens in wheat. *Science* 323, 1360–1363. doi: 10.1126/science.1166453
- Kretschmar, T., Kohlen, W., Sasse, J., Borghi, L., Schlegel, M., Bachelier, J. B., et al. (2012). A petunia ABC protein controls strigolactone-dependent symbiotic signalling and branching. *Nature* 483, 341–344. doi: 10.1038/nature10873
- Langowski, L., Ruzicka, K., Naramoto, S., Kleine-Vehn, J., and Friml, J. (2010). Trafficking to the outer polar domain defines the root-soil interface. *Curr. Biol.* 20, 904–908. doi: 10.1016/j.cub.2010.03.059
- Leljak-Levanic, D., Jezic, M., Cesar, V., Ludwig-Muller, J., Lepedus, H., Mladinic, M., et al. (2010). Biochemical and epigenetic changes in phytoplasma-recovered periwinkle after indole-3-butyric acid treatment. *J. Appl. Microbiol.* 109, 2069–2078. doi: 10.1111/j.1365-2672.2010.04837.x
- Lewis, D. R., and Muday, G. K. (2009). Measurement of auxin transport in *Arabidopsis thaliana*. *Nat. Protoc.* 4, 437–451. doi: 10.1038/nprot.2009.1
- Liu, X., Barkawi, L., Gardner, G., and Cohen, J. D. (2012). Transport of indole-3-butyric acid and indole-3-acetic acid in *Arabidopsis* hypocotyls using stable isotope labeling. *Plant Physiol.* 158, 1988–2000. doi: 10.1104/pp.111.191288
- Lu, X., Dittgen, J., Pislewska-Bednarek, M., Molina, A., Schneider, B., Svatos, A., et al. (2015). Mutant allele-specific uncoupling of PENETRATION3 functions reveals engagement of the ATP-binding cassette transporter in distinct tryptophan metabolic pathways. *Plant Physiol.* 168, 814–827. doi: 10.1104/pp.15.00182
- Ludwig-Muller, J. (2007). Indole-3-butyric acid synthesis in ecotypes and mutants of *Arabidopsis thaliana* under different growth conditions. *J. Plant Physiol.* 164, 47–59. doi: 10.1016/j.jplph.2005.10.008
- Mao, H., Aryal, B., Langenecker, T., Hagmann, J., Geisler, M., and Grebe, M. (2017). *Arabidopsis* BTB/POZ protein-dependent PENETRATION3 trafficking and disease susceptibility. *Nat. Plants* 3, 854–858. doi: 10.1038/s41477-017-0039-z
- Mao, H., Nakamura, M., Viotti, C., and Grebe, M. (2016). A framework for lateral membrane trafficking and polar tethering of the PEN3 ATP-binding cassette transporter. *Plant Physiol.* 172, 2245–2260. doi: 10.1104/pp.16.01252
- Matern, A., Böttcher, C., Eschen-Lippold, L., Westermann, B., Smolka, U., Döll, S., et al. (2019). A substrate of the ABC transporter PEN3 stimulates bacterial flagellin (flg22)-induced callose deposition in *Arabidopsis thaliana*. *J. Biol. Chem.* 294:jbc.RA119.007676. doi: 10.1074/jbc.RA119.007676
- Novak, O., Henykova, E., Sairanen, I., Kowalczyk, M., Pospisil, T., and Ljung, K. (2012). Tissue-specific profiling of the *Arabidopsis thaliana* auxin metabolome. *Plant J.* 72, 523–536. doi: 10.1111/j.1365-313X.2012.05085.x
- Ottenschlager, I., Wolff, P., Wolvert, C., Bhalerao, R. P., Sandberg, G., Ishikawa, H., et al. (2003). Gravity-regulated differential auxin transport from columella to lateral root cap cells. *Proc. Natl. Acad. Sci. U.S.A.* 100, 2987–2991. doi: 10.1073/pnas.04379361000437936100
- Rashotte, A. M., Poupart, J., Waddell, C. S., and Muday, G. K. (2003). Transport of the two natural auxins, indole-3-butyric acid and indole-3-acetic acid, in *Arabidopsis*. *Plant Physiol.* 133, 761–772. doi: 10.1104/pp.103.022582
- Ruzicka, K., Strader, L. C., Bailly, A., Yang, H., Blakeslee, J., Langowski, L., et al. (2010). *Arabidopsis* PIS1 encodes the ABCG37 transporter of auxinic compounds including the auxin precursor indole-3-butyric acid. *Proc. Natl. Acad. Sci. U.S.A.* 107, 10749–10753. doi: 10.1073/pnas.1005878107
- Schlicht, M., Ludwig-Muller, J., Burbach, C., Volkmann, D., and Baluska, F. (2013). Indole-3-butyric acid induces lateral root formation via peroxisome-derived indole-3-acetic acid and nitric oxide. *New Phytol.* 200, 473–482. doi: 10.1111/nph.12377
- Snider, J., Hanif, A., Lee, M. E., Jin, K., Yu, A. R., Graham, C., et al. (2013). Mapping the functional yeast ABC transporter interactome. *Nat. Chem. Biol.* 9, 565–572. doi: 10.1038/nchembio.1293
- Stein, M., Dittgen, J., Sanchez-Rodriguez, C., Hou, B. H., Molina, A., Schulze-Lefert, P., et al. (2006). *Arabidopsis* PEN3/PDR8, an ATP binding cassette transporter, contributes to nonhost resistance to inappropriate pathogens that enter by direct penetration. *Plant Cell* 18, 731–746. doi: 10.1105/tpc.105.038372
- Strader, L. C., and Bartel, B. (2008). A new path to auxin. *Nat. Chem. Biol.* 4, 337–339. doi: 10.1038/nchembio0608-337
- Strader, L. C., and Bartel, B. (2009). The *Arabidopsis* PLEIOTROPIC DRUG RESISTANCE8/ABCG36 ATP binding cassette transporter modulates sensitivity to the auxin precursor indole-3-butyric acid. *Plant Cell* 21, 1992–2007. doi: 10.1105/tpc.109.065821
- Strader, L. C., and Bartel, B. (2011). Transport and metabolism of the endogenous auxin precursor indole-3-butyric acid. *Mol. Plant* 4, 477–486. doi: 10.1093/mp/ssr006
- Strader, L. C., Monroe-Augustus, M., Rogers, K. C., Lin, G. L., and Bartel, B. (2008). *Arabidopsis* iba response5 suppressors separate responses to various hormones. *Genetics* 180, 2019–2031. doi: 10.1534/genetics.108.091512
- Underwood, W., and Somerville, S. C. (2017). Phosphorylation is required for the pathogen defense function of the *Arabidopsis* PEN3 ABC transporter. *Plant Signal. Behav.* 12:e1379644. doi: 10.1080/15592324.2017.1379644
- Xin, X. F., Nomura, K., Underwood, W., and He, S. Y. (2013). Induction and suppression of PEN3 focal accumulation during *Pseudomonas syringae* pv. tomato DC3000 infection of *Arabidopsis*. *Mol. Plant Microbe Interact.* 26, 861–867. doi: 10.1094/MPMI-11-12-0262-R
- Ziegler, J., Schmidt, S., Strehmel, N., Scheel, D., and Abel, S. (2017). *Arabidopsis* transporter ABCG37/PDR9 contributes primarily highly oxygenated coumarins to root exudation. *Sci. Rep.* 7:3704. doi: 10.1038/s41598-017-03250-6
- Zolman, B. K., Martinez, N., Millius, A., Adham, A. R., and Bartel, B. (2008). Identification and characterization of *Arabidopsis* indole-3-butyric acid response mutants defective in novel peroxisomal enzymes. *Genetics* 180, 237–251. doi: 10.1534/genetics.108.090399
- Zolman, B. K., Silva, I. D., and Bartel, B. (2001). The *Arabidopsis* pxa1 mutant is defective in an ATP-binding cassette transporter-like protein required for peroxisomal fatty acid beta-oxidation. *Plant Physiol.* 127, 1266–1278. doi: 10.1104/pp.127.3.1266

Conflict of Interest Statement: The authors declare that the research was conducted in the absence of any commercial or financial relationships that could be construed as a potential conflict of interest.

Copyright © 2019 Aryal, Huynh, Schneuwly, Siffert, Liu, Alejandro, Ludwig-Müller, Martinoia and Geisler. This is an open-access article distributed under the terms of the Creative Commons Attribution License (CC BY). The use, distribution or reproduction in other forums is permitted, provided the original author(s) and the copyright owner(s) are credited and that the original publication in this journal is cited, in accordance with accepted academic practice. No use, distribution or reproduction is permitted which does not comply with these terms.